

Article

# Application of Photocatalytic Falling Film Reactor to Elucidate the Degradation Pathways of Pharmaceutical Diclofenac and Ibuprofen in Aqueous Solutions

Kosar Hikmat Hama Aziz <sup>1,2,3,\*</sup> , Khalid M. Omer <sup>1,2</sup> , Ali Mahyar <sup>3</sup>, Hans Miessner <sup>3</sup>, Siegfried Mueller <sup>3</sup> and Detlev Moeller <sup>3</sup>

<sup>1</sup> Department of Chemistry, College of Science, University of Sulaimani, Qlyasan Street, Sulaimani City 46001, Kurdistan Region, Iraq

<sup>2</sup> Komar research Center (KRC), Komar University of Science and Technology, Sulaimani City 46001, Kurdistan Region, Iraq

<sup>3</sup> Laboratory of Atmospheric Chemistry and Air Quality, Brandenburg University of Technology (BTU Cottbus-Senftenberg), D-12489 Berlin, Germany

\* Correspondence: kosar.hamaaziz@univsul.edu.iq

Received: 20 May 2019; Accepted: 28 June 2019; Published: 25 July 2019



**Abstract:** Diclofenac (DCF) and ibuprofen (IBP) are common pharmaceutical residues that have been detected in the aquatic system. Their presence in the aquatic environment has become an emerging contaminant problem, which has implications for public health. The degradation pathway and identification of transformation products of pharmaceutical residues are crucial to elucidate the environmental fate of photocatalytic decomposition of these pollutants in aqueous media. The degradation process might lead to creation of other possible emerging contaminants. In this study, the degradation of DCF and IBP in aqueous solutions was investigated. To this end, coated TiO<sub>2</sub> on a Pilkington Active glass was used as a photocatalyst under UVA illumination, in a planar falling film reactor. Pilkington Activ<sup>TM</sup> glass was used as a photocatalyst and a falling liquid film generator. Degradation kinetics of both pharmaceuticals followed a pseudo-first-order model. The transformation products of both diclofenac and ibuprofen during the degradation process were detected and identified with gas chromatography–mass spectrometry (GC–MS) and ion chromatography. The results showed that the mineralization rate of both pharmaceuticals through photocatalysis was very low. Low chain carboxylic acids, such as formic, acetic, oxalic, malonic, and succinic acids were the main by-products. A pathway of DCF and IBP degradation was proposed.

**Keywords:** photocatalysis; titanium dioxide; diclofenac; ibuprofen; Pilkington active glass; degradation pathway

## 1. Introduction

Pharmaceutical wastes such as anthropogenic contaminants often cannot be easily removed using conventional wastewater treatment and thus accumulate in aquatic media [1,2]. Trace level of pharmaceutical residues have been detected in ground and surface water, which are considered a threat to the environment due to the high public consumption and continuous discharge to the water environment [3–6]. The accumulation of pharmaceuticals in aquatic environment, even in low concentrations, can be harmful for human health and aquatic life, resulting in a serious environmental problem [7,8]. Diclofenac (DCF) and ibuprofen (IBP) are highly consumed pharmaceuticals and are typical representatives of analgesic non-steroidal anti-inflammatory pharmaceutical compounds

(NSAIDs) that have been detected in water environment at low concentrations (ng/L to µg/L) [4,9–11]. NSAIDs are considered to be one of the most frequently detected pharmaceuticals in aquatic systems, including surface and ground water [12,13]. Advanced oxidation processes (AOPs) have attracted significant attention in the field of water treatment, due to its high removal efficiency and environmental compatibility [14]. Various AOPs have been successfully applied for environmental remediation [15,16] and have been safely and efficiently used for the removal of different organic contaminants, such as pharmaceuticals [4], herbicides [3] and organic dye [17], from aqueous solutions. AOPs are considered to be an effective and promising method for the degradation and mineralization of aqueous recalcitrant pharmaceutical compounds [2]. Different AOPs and their combinations have been compared and investigated for the removal of chloroacetic acids from aqueous solutions, using the design of a planar falling film reactor [14]. The same design of reactor have been applied for the removal of perfluorosurfactants through non-thermal plasma generated in a dielectric barrier discharge [18]. In order to mitigate the risks of these pollutants in a water environment, various AOPs have been examined for DCF and IBP removal [10]. Different advanced oxidation systems, such as ozonation, photolysis, photocatalysis, and their combinations have been investigated for the decomposition of DCF [19–21]. Photocatalysis is well-reported in literature for organic pollutants degradation in water environment, under visible and UV light irradiation. Degradation of DCF has also been studied in several reports using the commercial Pd/Al<sub>2</sub>O<sub>3</sub> [22], pyrite nanoparticles synthesized by sonication [23], photoelectrocatalysis under visible light irradiation [24], ozone and peroxone processes [25], heterogeneous photocatalysts [26,27], water radiolysis [28], gamma ray irradiation [29], electron beam irradiation [30], and Co<sub>3</sub>O<sub>4</sub>-CeO<sub>2</sub> as a heterogeneous catalyst for activation of persulfate [31].

IBP has already been treated by several oxidation processes, including Fenton oxidation using the Fe-ZSM5 catalyst [32], catalytic activation of peroxydisulfate by Fe<sub>3</sub>C embedded on carbon [33], and visible photodegradation using sustainable metal free-hybrids based on carbon nitride and biochar [11]. Choina et al. studied photocatalytic degradation of ibuprofen over titania catalysts [34]. Using heterogeneous photocatalyst TiO<sub>2</sub>/UV-LED [35], Zr-doped titania [36], and TiO<sub>2</sub>-NH<sub>2</sub>, nanoparticles have been investigated under visible light irradiation [37]. Photochemical transformation of ibuprofen into harmful 4-isobutylacetophenone was studied in [38]. Michael et al. proposed a degradation pathway of diclofenac and ibuprofen during sono-photocatalysis [39].

Identification of transformation products during the degradation of organic pollutants such as pharmaceutical residues is considered to be a big challenge. The quantity and type of these transformation products depend on the conditions of the treatment method. Identification of intermediates and mechanism pathway of photocatalytic degradation are considered to be an important step to control the oxidation process and to know the health effect of each transformation product [4,17].

This work aimed at systematically investigating the effect of photocatalytic oxidation on the degradation of DCF and IBP, using a planar falling film reactor. The planar falling film reactor has good merits of high reaction contact between the polluted solution and the coated photocatalyst on Pilkington active glass, which enhances the degradation efficiency due to the large surface-to-volume ratio in a falling liquid film system. Each intermediate was detected, identified, and quantified in order to develop a plausible degradation pathway for each substrate.

## 2. Materials and Methods

### 2.1. Materials

Diclofenac and ibuprofen sodium salts were purchased from Alfa Aesar (98.5%, Ward Hill, MA, USA) and Fluka (98%, Loughborough, UK), respectively. The chemicals and solvents used in this research were of high purity and were used as received. All solutions were prepared in deionized water.

## 2.2. Experimental Setup and Procedure

The photocatalytic experiments were conducted in a planar falling film reactor (Figure 1); described in detail in [14,17]. Briefly, the reactor was composed of two Pilkington Activ™ glass (PAG) sheets that were used without any further preparation processes, and were connected by a frame of PVC. PAG is a thin (4–6 mm thickness), colorless, and transparent glass sheet of TiO<sub>2</sub> nanoparticles with an anatase crystalline structure and an average crystalline size of 18 nm and a mean grain size of 95 nm that are coated as a nano-layer (12–15 nm) on the surface of glass [40]. Application of PAG in this falling film reactor provided a good wettability on the surface of the reactor walls, owing to the high superhydrophilicity ( $\theta_c = 0^\circ$ ,  $\theta_c$ —water contact angle) of the TiO<sub>2</sub> photocatalyst coated on the PAG, resulting in the formation of a stable homogeneous falling liquid film (~150  $\mu\text{m}$  thickness) along the glass sheets. Seven UVA lamps (NARVA Lichtquellen GmbH, Brand-Erbisdorf, Germany, model LT 15 W/009 UV, each with 15 W energy consumption) were placed inside the reactor, which had a maximum wavelength of 360 nm, for the UVA irradiation. The UV light intensity was measured as 1 mW/cm<sup>2</sup> at  $\lambda_{\text{max}} = 360$  nm. There was no significant aging effect during the experimental period. In all experiments, the reactor was charged with the solution volume of 0.5 L DCF or IBP (initial concentration = 50 mg/L). The use of such high concentrations in the present work was to ensure adequate detection of transformation products by gas chromatography–mass spectrometry (GC–MS, Agilent, Santa Clara, CA, USA). After establishing a homogeneous liquid falling film flow through the PAG sheets, the solution was continuously circulated into the reactor using a gear pump (Ismatec Reglo-z Digital, Wertheim, Germany), with a flow rate of 1 L/min. During the experiments, oxygen was continuously flown into the reactor at flow rate of 10 L/h (controlled by a Brooks Mass Flow Controller 5850E, Hatfield, PA, USA). The concentration of the dissolved oxygen in the liquid phase and the temperature of the treated solution were monitored using an electrochemical sensor Hach Orbisphere 410 (A1100, Düsseldorf, Germany).

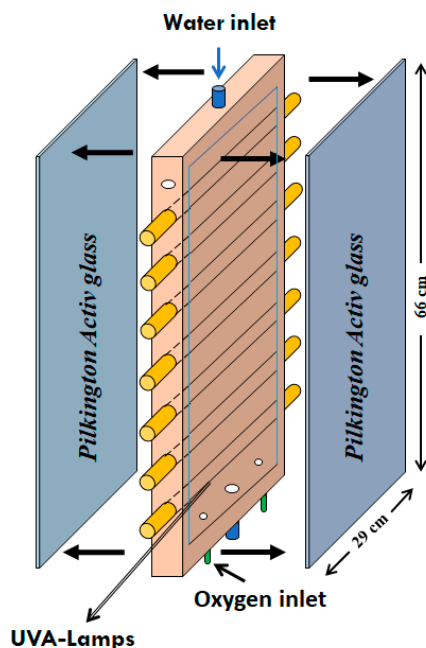


Figure 1. Schematic diagram of the photocatalytic reactor.

## 2.3. Average Thickness of the Liquid Falling Film

Among the various methods of measuring the average liquid film thickness, the simplest method is collecting and measuring the volume of the distinct amount of the liquid that has flown down the surface of the reactor [41]. The average thickness of the liquid falling film was calculated by dividing the average volume of the water collected by the surface area of the reactor wall. Due to the difficulty of

disassembling the planar reactor used for collecting the exact amount of the drained water, and because the collected water from the outlet of the reactor was not accurate, the same technique was applied with a small modification. The thickness of the liquid falling film in the planar reactor was calculated according to the following equation (Equation (1)):

$$\sigma = \frac{Q \times t}{A} \times 10^4 \quad (1)$$

where  $\sigma$  ( $\mu\text{m}$ ) is the average liquid film thickness,  $Q$  ( $\text{cm}^3/\text{s}$ ) is the liquid flow rate,  $t$  is the time (in second) required for water to cover the whole surface area of the reactor wall, and  $A$  (in  $\text{cm}^2$ ) is the total surface area of the reactor wall covered by the liquid falling film.  $A$  and  $Q$  were constant throughout the experiment,  $Q$  was controlled by the gear pump, while  $A$  was calculated from the surface area of two Pilkington glass sheets (29 cm  $\times$  68 cm). The required time ( $t$ ) for covering all of the Pilkington surface area with the liquid was measured by the stopwatch; this was repeated several times. The obtained liquid film thickness was  $145 \pm 5 \mu\text{m}$  for 500 mL of water circulated at a flow rate of 1 L/min, in the planar falling film reactor.

#### 2.4. Analysis

The concentrations of DCF and IBP were measured using HPLC (Gynkotek HPLC system (Dionex, Berlin, Germany equipped with a M480G gradient pump, GINA 50 Autosampler, and UVD 1705 Dual-Channel UV-VIS Detector) at 254 and 230 nm, respectively. The stationary phase was a NUCLEOSIL 100-5 C18 (125 mm  $\times$  2 mm, 5  $\mu\text{m}$ ) column, while the mobile phase consisted of 50% Acetonitrile and (50% of 0.01% acetic acid (HAC) for DCF and 1% HAC for IBP) ultra-pure water at a 250  $\mu\text{L}/\text{min}$  flow rate. The release of low chain anionic by-products, such as acetate, oxalate, chloride, nitrate, maleate, malonate and succinate, from DCF and IBP, during the degradation process, were quantified by ion chromatography, using a Dionex DX 500 (Thermo Fisher, Berlin, Germany equipped with a CD20 conductivity detector connected to an IonPac AS14 (4  $\times$  250 mm) column and an AG14 (guard column). The mobile phase consisted of a mixture of  $\text{NaHCO}_3$  (1.0 mM) and  $\text{Na}_2\text{CO}_3$  (3.5 mM), flowing with 1.2 mL/min.

The transformation products formed during the degradation of diclofenac and ibuprofen were identified by gas chromatography–mass spectrometry (GC–MS). An Agilent (GC: 6890, MS: 5975) was equipped with a capillary column DB-5MS (10 m  $\times$  0.25 mm ID  $\times$  0.1  $\mu\text{m}$  film thickness). The carrier gas was helium at a flow rate of 6.0 mL/minute. The GC–MS system was operated in an electron impact ionization scan mode using the NIST14 spectra library. The analysis was performed by PiCA Prüfinstitut Chemische Analytik GmbH, Berlin, Germany. Each sample was analyzed by both an acidic and alkaline extraction procedure with a Methyl tert-butyl ether (MTBE) solvent, after being spiked with an internal standard (i.a.PCB209) solution. The degree of mineralization of both pollutants was followed by a total organic carbon (TOC) analysis, using a Shimadzu TOC-5000 (Kyoto, Japan) analyzer.

### 3. Results and Discussion

#### 3.1. Photocatalytic Mechanism and Superhydrophilicity of $\text{TiO}_2$

Despite the large variety of photocatalysts reported in literature, which showed a capability for decomposing and mineralizing various organic pollutants, the  $\text{TiO}_2$  anatase/rutile heterostructure as a photocatalyst has been successfully commercialized and its use is widespread. The principle of  $\text{TiO}_2$  photocatalysis in the degradation process is based on the photo-generated electron-hole pair (Equation (2)). When a semiconductor is illuminated with light of sufficient energy ( $>$ band gap energy) it produces highly reactive species like hydroxyl and superoxide radicals, which can cause a photocatalytic degradation of pollutants. In order to achieve successful and continuous production of reactive oxidizing chemical species, as well as prevent electron-hole recombination, two redox reactions must occur simultaneously. The first one includes the reduction of the adsorbed electrophilic

dissolved oxygen molecule on the TiO<sub>2</sub>, through photo-generated electrons, to form superoxide anion radicals (Equation (3)) that might further react with H<sup>+</sup> to generate hydroperoxyl radicals (Equation (4)), followed by H<sub>2</sub>O<sub>2</sub>, and finally, hydroxyl radicals (Equations (5) and (6)). The second one involves oxidation of the adsorbed water molecule or hydroxyl anions by photo-generated holes, to produce hydroxyl radicals (Equation (7)). The powerful hydroxyl and superoxide anion radicals could subsequently oxidize and mineralize organic pollutants into CO<sub>2</sub>, H<sub>2</sub>O, and mineral salts (Equations (8)–(10)) [42].



Exposure of a surface coated with TiO<sub>2</sub> nanoparticles to UV light could generate superhydrophilicity on the illuminated surface, which has been well-described by Fujishima et al. [43]. This superhydrophilicity results in a high wettability over the surface of TiO<sub>2</sub> coated material, which is particularly used in the production of anti-fogging and self-cleaning glasses [42]. In this phenomenon, the photo-generated electron-hole pairs react in a different route. The electrons tend to reduce the Ti(IV) to the Ti(III) state, and the holes oxidize the O<sup>2-</sup> anions to O<sub>2</sub>. The strength of the bond between the associated titanium and the lattice oxygen is reduced by these trapped holes, resulting in the release of oxygen atoms that can lead to oxygen vacancies (Figure 2). Water molecules can then be adsorbed and settled in these oxygen vacancies as OH groups that make the surface hydrophilic. The longer illumination of the surface with UV light reduces the water contact angle of water. When the contact angle approaches zero, water has the tendency to spread perfectly across the surface [43]. This phenomenon of TiO<sub>2</sub> coated on the surface of PAG (reactor walls), provides a stable and homogeneous liquid flow in the falling film reactor.

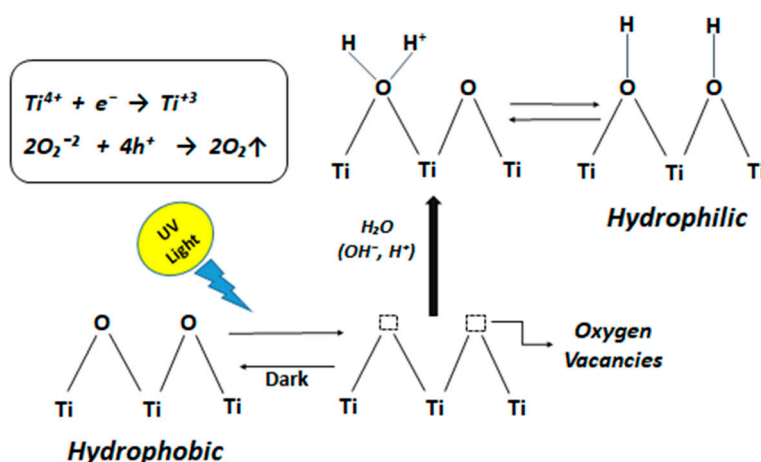
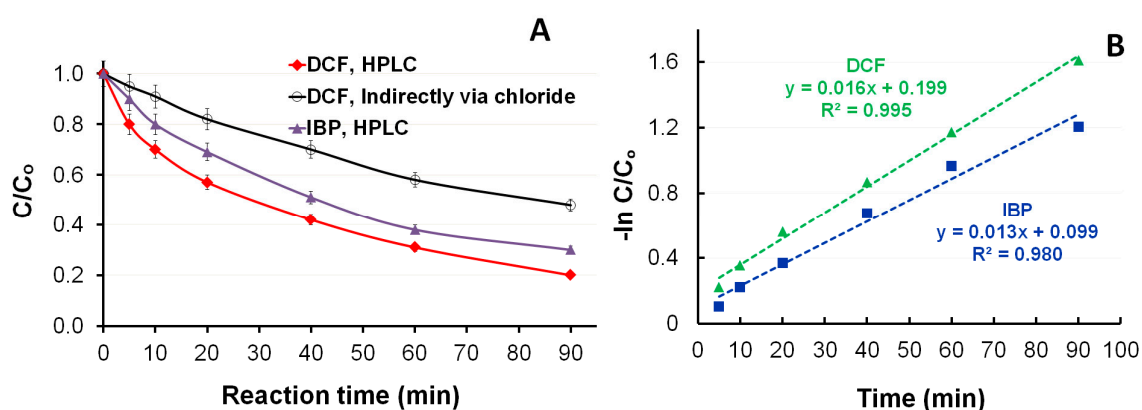


Figure 2. Mechanism of photo-induced superhydrophilicity of TiO<sub>2</sub>.

### 3.2. Photocatalytic Degradation of DCF and IBP

Control experiments in the dark were conducted in order to test the contribution of the adsorption processes in the removal efficiency. The concentration of 50 mg/L DCF and IBP remained constant after 90 min of circulation, indicating that the adsorption processes were not involved in the removal process. The photocatalytic degradation profiles of both pharmaceuticals are shown in Figure 3; the measured chloride ions in the treated solution were used as indirect measurement for DCF degradation. As shown in Figure 3A, once the solution of DCF was subjected to the photocatalytic degradation, chloride anions were released, as detected by ion chromatography. The rate constants were calculated by plotting  $\ln(C_0/C)$  versus time ( $t$ ), as shown in Figure 3B and the linearity of the plots confirmed pseudo-first-order kinetics for the degradation of both pharmaceuticals.



**Figure 3.** (A) Relative concentration profiles of diclofenac (DCF) and ibuprofen (IBP) degradation. (B) Observed removal rate constants ( $K \text{ min}^{-1}$ ) (initial Concentration = 50 mg/L, 0.5 L, pH = 5).

To investigate the mineralization of DCF and IBP under photocatalysis, the concentration of TOC after a 90-min treatment was measured. It was found that the TOC% removal for 50 mg/L of the initial concentration of DCF and IBP and 0.5 L solution after a 90-min treatment were 16.0% and 15.3%, respectively.

### 3.3. Degradation Products and Pathways

Advanced oxidation processes based on the use of  $\text{TiO}_2$  under UVA illumination for the degradation of pharmaceutical pollutants produced numerous transformation products, since the generated hydroxyl radicals did not exhibit selectively towards various functional groups. Other generated reactive species, such as superoxide radicals and photo-generated electron-hole pairs, participated in various oxidation reduction pathways as well [39]. The  $m/z$  ratio obtained from the GC-MS, the proposed formulae and structures for the intermediates of both pharmaceuticals—DCF and IBP—are shown in Tables 1 and 2. The results of the GC-MS chromatograms are shown in the Supplementary Materials. The proposed degradation pathway were also further consolidated using the results obtained from ion chromatography (IC), for identification of several low chain carboxylic acids. A number of chemical processes have been identified during the degradation of DCF and IBP, by AOPs, including hydroxylation, dechlorination, decarboxylation, cyclization, and ring-opening reactions, followed by the formation of organic aliphatic by-products (Tables 1 and 2). Hydroxylated by-products are considered to be the main degradation intermediates. A possible photocatalytic degradation reaction pathway for DCF and IBP, based on the results obtained by GC-MS and ion chromatography have been proposed; shown in Figures 4 and 5, respectively.

**Table 1.** Identified intermediate by-products during photocatalytic degradation of DCF. *m/z*—mass to charge ratio and *R<sub>t</sub>*—retention time obtained from the gas chromatography–mass spectrometry (GC–MS).

Number	Compounds	<i>m/z</i>	<i>R<sub>t</sub></i> (min)
(1)	Diclofenac	295.1	12.929
(2)	[2-(2,6-Dichlorophenylamino)-phenyl]-hydroxy-acetic acid	311	11.334
(3)	Dihydroxylation diclofenac	327.1	13.664
(4)	2-(2,6-Dichlorophenylamino)-benzaldehyde	265.1	11.294
(5)	2-(2-Chlorophenylamino)-benzaldehyde	231.1	10.777
(6)	1-(2,6-Dichlorophenyl)-1,3-dihydro-2H-endol-2-one	277.1	11.868
(7)	2-[2-(2-chloro-6-hydroxy anilino)phenyl]acetic acid	277.1	11.868
(8)	1-(2,6-Dichlorophenyl)-3-hydroxyindolin-2-one	293.1	13.392
(9)	1-(2,6-Dichlorophenyl)-5-hydroxyindolin-2-one	293.1	13.964
(10)	1-(2,6-Dichlorophenyl)-7-hydroxyindolin-2-one	293.1	14.467
(11)	1-(2,6-Dichloro-4-hydroxyphenyl)indolin-2-one	293.1	13.39
(12)	1-(2,6-Dichlorophenyl)-1H-benzo [1,2] oxazine-3-4H-one	293.1	13.964
(13)	N-(2,6-Dichlorophenyl)-2-formylbenzamide	293.1	14.467
(14)	2,6-Dichloroaniline	161	5.068
(15)	2,6-Dichlorobenzonitrile	171	5.314
(16)	2,6-Dichlorophenol	162	4.768

**Table 2.** Identified intermediate by-product during photocatalytic degradation of IBP.

Number	Compounds	<i>m/z</i>	<i>R<sub>t</sub></i> (min)
(1)	Ibuprofen	206.1	8.65
(2)	2-Hydroxy-2-(4-(1-hydroxy-2-methylpropyl)phenyl)propanoic acid	235.1	7.140
(3)	4-Isobutylbenzoic acid	178	6.704
(4)	4-Isobutylbenzaldehyde	162	6.063
(5)	4-Isopropylbenzaldehyde	148	4.636
(6)	4-Ethylacetophenone	148	6.165
(7)	4-Isobutylacetophenone	176	6.690
(8)	4-(1-carboxyethyl)benzoic acid	190	8.140

In order to identify the intermediates and to understand the degradation pathway of DCF and IBP during photocatalytic treatments, samples have been collected at various treatment times (after 5, 15, 30, 60, and 90 min photocatalytic treatment). The intermediate products of both pharmaceuticals DCF and IBP produced during photocatalytic degradation were identified by GC–MS; presented in Tables 1 and 2. The short chain acids such as formate, acetate, oxalate, maleate, malonate, and succinate, were identified through ion-chromatography. Figure 4 illustrates a plausible degradation pathway of DCF through the photocatalysis treatment. The degradation pathway was based on the results presented in Table 1. The aromatic rings of the intermediate compounds (Figures 4 and 5) broke into different cleavage compounds through the generated hydroxyl radicals, followed by organic acids like carboxylic and aliphatic acids. These non-toxic and harmless acids further oxidized in the presence of hydroxyl radicals and produced carbon dioxide and water.

The results of the GC–MS indicated that a number of by-products (listed in Table 2) were identified during the photocatalytic degradation of IBP. Based on the results showed in Table 2 and the short chain acids, such as formate, acetate, oxalate, and malonate, which were identified through ion-chromatography, a photocatalytic degradation pathway of IBP were proposed (Figure 5).

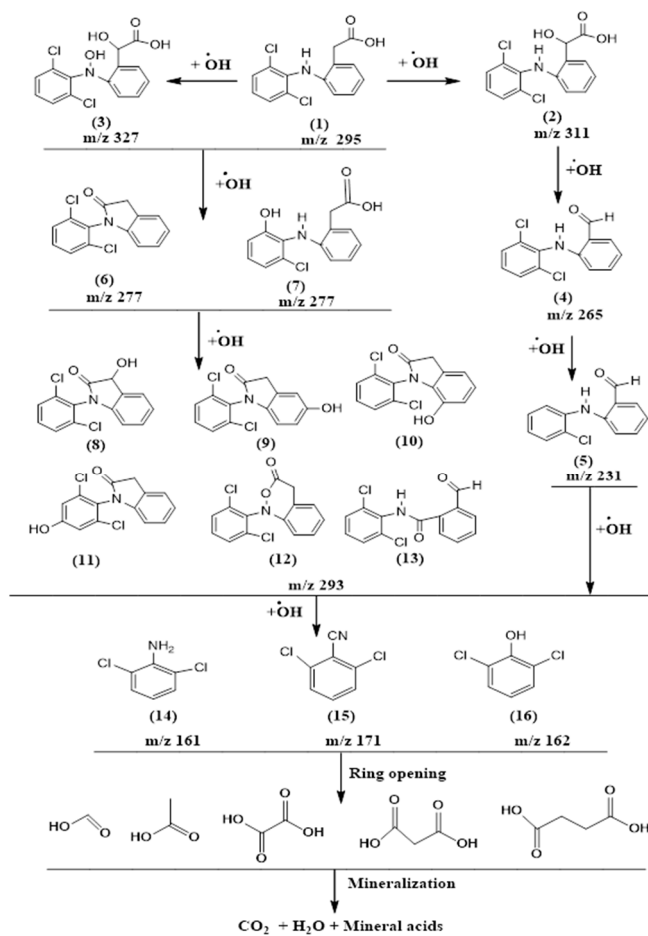


Figure 4. Proposed degradation pathways of DCF through photocatalysis.

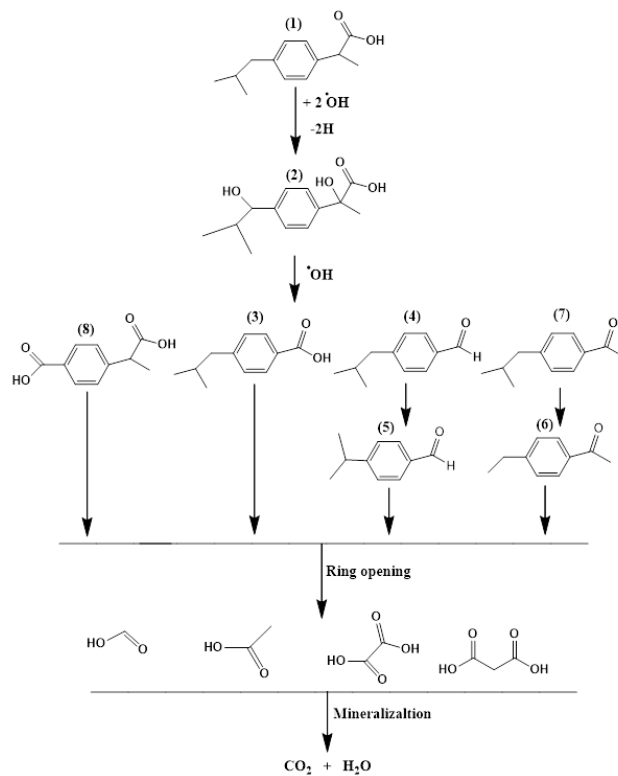


Figure 5. Proposed degradation pathways of IBP through photocatalysis.

#### 4. Conclusions

In summary, a number of photocatalytic intermediates of pharmaceutical DCF and IBP were detected and identified under UVA illumination of Pilkington active glass using falling film reactor. Photocatalytic degradation pathways of two common pharmaceutical pollutants in the system were proposed. This study might lead to better understanding of the photocatalytic degradation pathways of DCF and IBP in aqueous solutions and the fate of transformation products. The first step in the degradation of pharmaceuticals, under photocatalytic treatment, is the hydroxylation, decarboxylation, and cleavage of the carbon–carbon or carbon–nitrogen bond via generated hydroxyl radicals, followed by further oxidation and ring-opening with formation of several low-chain carboxylic acids, like formic, acetic, oxalic, malonic, and succinic acids. The use of photocatalysis has a very low mineralization rate and is not feasible to completely remove DCF and IBP, as it requires a high reaction time. However, it was found to be effective for degradation of recalcitrant organic pollutants like pharmaceutical residues or, at least, to transform them into biodegradable species. Therefore, for a deeper mineralization, a longer exposure time during photocatalysis, before discharging these pollutants into the aquatic system, is essential.

**Supplementary Materials:** The following are available online at <http://www.mdpi.com/2079-6412/9/8/465/s1>, Figure S1: GC–MS chromatogram obtained for the photocatalytic degradation of DCF (50 mg/L) under UVA irradiation. The identified degradation intermediates are shown in Table 1; Figure S2: GC–MS chromatogram obtained for photocatalytic degradation of IBP (50 mg/L) under UVA irradiation. The identified degradation intermediates are shown in Table 2.

**Author Contributions:** Conceptualization, K.H.H.A., H.M., S.M., and D.M.; Investigation, K.H.H.A. and A.M.; Methodology, K.H.H.A. and A.M.; Writing–Review & Editing, K.H.H.A., K.M.O., A.M., and D.M.

**Funding:** This work was funded by the German Federal Ministry of Economic Affairs and Energy (BMW, No. KF3216203 RH4).

**Acknowledgments:** The author thanks the University of Sulaimani, Kurdistan-Iraq and the institute for Atmospheric Chemistry and Air Pollution Control, Brandenburg University of Technology (BTU Cottbus-Senftenberg), D-12489 Berlin, Germany for supporting this work.

**Conflicts of Interest:** The authors declare no conflict of interest.

#### References

1. Banaschik, R.; Jablonowski, H.; Bednarski, P.J.; Kolb, J.F. Degradation and intermediates of diclofenac as instructive example for decomposition of recalcitrant pharmaceuticals by hydroxyl radicals generated with pulsed corona plasma in water. *J. Hazard. Mater.* **2018**, *342*, 651–660. [[CrossRef](#)] [[PubMed](#)]
2. Kanakaraju, D.; Glass, B.D.; Oelgemöller, M. Advanced oxidation process-mediated removal of pharmaceuticals from water: A review. *J. Environ. Manag.* **2018**, *219*, 189–207. [[CrossRef](#)] [[PubMed](#)]
3. Aziz, K.H.H.; Miessner, H.; Mueller, S.; Mahyar, A.; Kalass, D.; Moeller, D.; Khorshid, I.; Rashid, M.A.M. Comparative study on 2,4-dichlorophenoxyacetic acid and 2,4-dichlorophenol removal from aqueous solutions via ozonation, photocatalysis and non-thermal plasma using a planar falling film reactor. *J. Hazard. Mater.* **2018**, *343*, 107–115. [[CrossRef](#)] [[PubMed](#)]
4. Aziz, K.H.H.; Miessner, H.; Mueller, S.; Kalass, D.; Moeller, D.; Khorshid, I.; Rashid, M.A.M. Degradation of pharmaceutical diclofenac and ibuprofen in aqueous solution, a direct comparison of ozonation, photocatalysis, and non-thermal plasma. *Chem. Eng. J.* **2017**, *313*, 1033–1041. [[CrossRef](#)]
5. Klavarioti, M.; Mantzavinos, D.; Kassinos, D.; Fatta-Kassinos, D. Removal of residual pharmaceuticals from aqueous systems by advanced oxidation processes. *Environ. Int.* **2009**, *35*, 402–417. [[CrossRef](#)] [[PubMed](#)]
6. Ikehata, K.; Naghashkar, N.J.; El-Din, M.G. Degradation of Aqueous Pharmaceuticals by Ozonation and Advanced Oxidation Processes: A Review. *Ozone Sci. Eng.* **2006**, *28*, 353–414. [[CrossRef](#)]
7. Hernando, M.D.; Heath, E.; Petrovic, M.; Barceló, D. Trace-level determination of pharmaceutical residues by LC-MS/MS in natural and treated waters. A pilot-survey study. *Anal. Bioanal. Chem.* **2006**, *385*, 985–991. [[CrossRef](#)]

8. Luo, Y.; Guo, W.; Ngo, H.H.; Nghiem, L.D.; Hai, F.I.; Zhang, J.; Liang, S.; Wang, X.C. A review on the occurrence of micropollutants in the aquatic environment and their fate and removal during wastewater treatment. *Sci. Total. Environ.* **2014**, *473*, 619–641. [[CrossRef](#)]
9. Vieno, N.M.; Härkki, H.; Tuhkanen, T.; Kronberg, L. Occurrence of pharmaceuticals in river water and their elimination in a pilot-scale drinking water treatment plant. *Environ. Sci. Technol.* **2007**, *41*, 5077–5084. [[CrossRef](#)]
10. Zwiener, C. Oxidative treatment of pharmaceuticals in water. *Water Res.* **2000**, *34*, 1881–1885. [[CrossRef](#)]
11. Kumar, A.; Sharma, G.; Naushad, M.; Al-Muhtaseb, A.H.; Kumar, A.; Hira, I.; Ahamad, T.; Ghfar, A.A.; Stadler, F.J. Visible photodegradation of ibuprofen and 2,4-D in simulated waste water using sustainable metal free-hybrids based on carbon nitride and biochar. *J. Environ. Manag.* **2019**, *231*, 1164–1175. [[CrossRef](#)] [[PubMed](#)]
12. Kanakaraju, D.; Motti, C.A.; Glass, B.D.; Oelgemöller, M.; Oelgemoeller, M. Photolysis and TiO<sub>2</sub>-catalysed degradation of diclofenac in surface and drinking water using circulating batch photoreactors. *Environ. Chem.* **2014**, *11*, 51–62. [[CrossRef](#)]
13. Rivera-Utrilla, J.; Sánchez-Polo, M.; Ferro-García, M.Á.; Prados-Joya, G.; Ocampo-Perez, R. Pharmaceuticals as emerging contaminants and their removal from water. A review. *Chemosphere* **2013**, *93*, 1268–1287. [[CrossRef](#)] [[PubMed](#)]
14. Aziz, K.H.H. Application of different advanced oxidation processes for the removal of chloroacetic acids using a planar falling film reactor. *Chemosphere* **2019**, *228*, 377–383. [[CrossRef](#)] [[PubMed](#)]
15. Cheng, M.; Zeng, G.; Huang, D.; Lai, C.; Xu, P.; Zhang, C.; Liu, Y. Hydroxyl radicals based advanced oxidation processes (AOPs) for remediation of soils contaminated with organic compounds: A review. *Chem. Eng. J.* **2016**, *284*, 582–598. [[CrossRef](#)]
16. Aziz, K.H.H.; Miessner, H.; Mahyar, A.; Mueller, S.; Kalass, D.; Moeller, D.; Omer, K.M. Removal of dichloroacetic acid from aqueous solution using non-thermal plasma generated by dielectric barrier discharge and nano-pulse corona discharge. *Sep. Purif. Technol.* **2019**, *216*, 51–57. [[CrossRef](#)]
17. Aziz, K.H.H.; Mahyar, A.; Miessner, H.; Mueller, S.; Kalass, D.; Moeller, D.; Khorshid, I.; Rashid, M.A.M. Application of a planar falling film reactor for decomposition and mineralization of methylene blue in the aqueous media via ozonation, Fenton, photocatalysis and non-thermal plasma: A comparative study. *Process. Saf. Environ. Prot.* **2018**, *113*, 319–329. [[CrossRef](#)]
18. Mahyar, A.; Miessner, H.; Mueller, S.; Aziz, K.H.H.; Kalass, D.; Moeller, D.; Kretschmer, K.; Manuel, S.R.; Noack, J. Development and application of different non-thermal plasma reactors for the removal of perfluorosurfactants in water: A comparative study. *Plasma Chem. Plasma Process.* **2019**, *39*, 531–544. [[CrossRef](#)]
19. Moreira, N.F.; Orge, C.A.; Ribeiro, A.R.; Faria, J.L.; Nunes, O.C.; Pereira, M.F.R.; Silva, A.M.; Pereira, M.F. Fast mineralization and detoxification of amoxicillin and diclofenac by photocatalytic ozonation and application to an urban wastewater. *Water Res.* **2015**, *87*, 87–96. [[CrossRef](#)]
20. Gou, J.; Ma, Q.; Cui, Y.; Deng, X.; Zhang, H.; Cheng, X.; Li, X.; Xie, M.; Cheng, Q.; Liu, H. Visible light photocatalytic removal performance and mechanism of diclofenac degradation by Ag<sub>3</sub>PO<sub>4</sub> sub-microcrystals through response surface methodology. *J. Ind. Eng. Chem.* **2017**, *49*, 112–121. [[CrossRef](#)]
21. Aguinaco, A.; Beltrán, F.J.; García-Araya, J.F.; Oropesa, A.L. Photocatalytic ozonation to remove the pharmaceutical diclofenac from water: Influence of variables. *Chem. Eng. J.* **2012**, *189*, 275–282. [[CrossRef](#)]
22. Nieto-Sandoval, J.; Munoz, M.; De Pedro, Z.M.; Casas, J.A. Fast degradation of diclofenac by catalytic hydrodechlorination. *Chemosphere* **2018**, *213*, 141–148. [[CrossRef](#)] [[PubMed](#)]
23. Khabbaz, M.; Entezari, M. Degradation of Diclofenac by sonosynthesis of pyrite nanoparticles. *J. Environ. Manag.* **2017**, *187*, 416–423. [[CrossRef](#)] [[PubMed](#)]
24. Cheng, X.; Wang, P.; Liu, H. Visible-light-driven photoelectrocatalytic degradation of diclofenac by N, S-TiO<sub>2</sub>/TiO<sub>2</sub> NTs photoelectrode: performance and mechanism study. *J. Environ. Chem. Eng.* **2015**, *3*, 1713–1719. [[CrossRef](#)]
25. Vogna, D.; Marotta, R.; Napolitano, A.; Andreozzi, R.; D’Ischia, M. Advanced oxidation of the pharmaceutical drug diclofenac with UV/H<sub>2</sub>O<sub>2</sub> and ozone. *Water Res.* **2004**, *38*, 414–422. [[CrossRef](#)] [[PubMed](#)]
26. Martínez, C.; Canle, M.; Fernandez, M.I.; Santaballa, J.A.; Faria, J. Aqueous degradation of diclofenac by heterogeneous photocatalysis using nanostructured materials. *Appl. Catal. B Environ.* **2011**, *107*, 110–118. [[CrossRef](#)]

27. Chianese, S.; Iovino, P.; Leone, V.; Musmarra, D.; Prisciandaro, M. Photodegradation of diclofenac sodium salt in water solution: Effect of HA,  $\text{NO}_3^-$  and  $\text{TiO}_2$  on photolysis performance. *Water Air Soil Pollut.* **2017**, *228*, 270. [CrossRef]
28. Trojanowicz, M.; Bojanowska-Czajka, A.; Kciuk, G.; Bobrowski, K.; Gumiel, M.; Koc, A.; Naęcz-Jawecki, G.; Torun, M.; Ozbay, D. Application of ionizing radiation in decomposition of selected organic pollutants in waters. *Eur. Water* **2012**, *39*, 15–26.
29. Liu, Q.; Luo, X.; Zheng, Z.; Zheng, B.; Zhang, J.; Zhao, Y.; Yang, X.; Wang, J.; Wang, L. Factors that have an effect on degradation of diclofenac in aqueous solution by gamma ray irradiation. *Environ. Sci. Pollut. Res.* **2011**, *18*, 1243–1252. [CrossRef]
30. Tominaga, F.K.; Batista, A.P.D.S.; Teixeira, A.C.S.C.; Borrelly, S.I. Degradation of diclofenac by electron beam irradiation: Toxicity removal, by-products identification and effect of another pharmaceutical compound. *J. Environ. Chem. Eng.* **2018**, *6*, 4605–4611. [CrossRef]
31. Xian, G.; Zhang, G.; Chang, H.; Zhang, Y.; Zou, Z.; Li, X. Heterogeneous activation of persulfate by  $\text{Co}_3\text{O}_4\text{-CeO}_2$  catalyst for diclofenac removal. *J. Environ. Manag.* **2019**, *234*, 265–272. [CrossRef] [PubMed]
32. Adityosulindro, S.; Julcour, C.; Barthe, L. Heterogeneous Fenton oxidation using Fe-ZSM5 catalyst for removal of ibuprofen in wastewater. *J. Environ. Chem. Eng.* **2018**, *6*, 5920–5928. [CrossRef]
33. Zhang, G.; Ding, Y.; Nie, W.; Tang, H. Efficient degradation of drug ibuprofen through catalytic activation of peroxymonosulfate by Fe<sub>3</sub>C embedded on carbon. *J. Environ. Sci.* **2019**, *78*, 1–12. [CrossRef] [PubMed]
34. Choina, J.; Kosslick, H.; Fischer, C.; Flechsig, G.-U.; Frunza, L.; Schulz, A. Photocatalytic decomposition of pharmaceutical ibuprofen pollutions in water over titania catalyst. *Appl. Catal. B Environ.* **2013**, *129*, 589–598. [CrossRef]
35. Jallouli, N.; Pastrana-Martínez, L.M.; Ribeiro, A.R.; Moreira, N.F.; Faria, J.L.; Hentati, O.; Silva, A.M.; Ksibi, M. Heterogeneous photocatalytic degradation of ibuprofen in ultrapure water, municipal and pharmaceutical industry wastewaters using a  $\text{TiO}_2/\text{UV-LED}$  system. *Chem. Eng. J.* **2018**, *334*, 976–984. [CrossRef]
36. Choina, J.; Fischer, C.; Flechsig, G.-U.; Kosslick, H.; Tuan, V.; Tuyen, N.; Tuyen, N.; Schulz, A. Photocatalytic properties of Zr-doped titania in the degradation of the pharmaceutical ibuprofen. *J. Photochem. Photobiol. A Chem.* **2014**, *274*, 108–116. [CrossRef]
37. Uheida, A.; Mohamed, A.; Belaqiz, M.; Nasser, W.S. Photocatalytic degradation of Ibuprofen, Naproxen, and Cetirizine using PAN-MWCNT nanofibers crosslinked  $\text{TiO}_2\text{-NH}_2$  nanoparticles under visible light irradiation. *Sep. Purif. Technol.* **2019**, *212*, 110–118. [CrossRef]
38. Ruggeri, G.; Ghigo, G.; Maurino, V.; Minero, C.; Vione, D. Photochemical transformation of ibuprofen into harmful 4-isobutylacetophenone: Pathways, kinetics, and significance for surface waters. *Water Res.* **2013**, *47*, 6109–6121. [CrossRef]
39. Michael, I.; Achilleos, A.; Lambropoulou, D.; Torrens, V.O.; Pérez, S.; Petrović, M.; Barceló, D.; Fatta-Kassinos, D. Proposed transformation pathway and evolution profile of diclofenac and ibuprofen transformation products during (sono) photocatalysis. *Appl. Catal. B Environ.* **2014**, *147*, 1015–1027. [CrossRef]
40. Mahyar, A.; Miessner, H.; Mueller, S.; Moeller, D. Empirical determination and modeling of ozone mass transfer in a planar falling film reactor. *Chem. Eng. Res. Des.* **2017**, *121*, 287–294. [CrossRef]
41. Mehrjouei, M.; Müller, S.; Möller, D. Design and characterization of a multi-phase annular falling-film reactor for water treatment using advanced oxidation processes. *J. Environ. Manag.* **2013**, *120*, 68–74. [CrossRef] [PubMed]
42. Pelaez, M.; Nolan, N.T.; Pillai, S.C.; Seery, M.K.; Falaras, P.; Kontos, A.G.; Dunlop, P.S.; Hamilton, J.W.; Byrne, J.; O’Shea, K.; et al. A review on the visible light active titanium dioxide photocatalysts for environmental applications. *Appl. Catal. B Environ.* **2012**, *125*, 331–349. [CrossRef]
43. Fujishima, A.; Rao, T.N.; Tryk, D.A. Titanium dioxide photocatalysis. *J. Photochem. Photobiol. C* **2000**, *1*, 1–21. [CrossRef]

